Robust Microwave Characterization of Inkjet Printed Coplanar Waveguides on Flexible Substrates

Abhishek Sahu, *Student Member, IEEE,* Peter H. Aaen, *Senior Member, IEEE,* Arkadiusz Lewandowski, *Member, IEEE,* Maxim Shkunov, Greg P. Rigas, Paul T. Blanchard, Thomas M. Wallis, *Member, IEEE,* and Vijay Devabhaktuni, *Senior Member, IEEE*

***Abstract*—In this paper, we propose a robust microwave characterization of inkjet printed components on flexible substrates, which aim at measuring the material properties of silver nanoparticle inks and the supporting dielectric spacer employed during measurements. Starting with propagation constant extracted from multiline thru-reflect-line calibration with coplanar waveguide (CPW) standards and then proceeding with finite element modeling of CPWs, the proposed technique can dynamically produce an interpolated search space by automatic driving of simulation tools. In the final stage, the algorithm utilizes a least-square optimization routine to minimize the deviation between model and measurements. Our technique significantly reduces the computing resources and is able to extract the material parameters using even a nominal ink profile. Characteristic impedances for CPWs are extracted using series resistor measurements from 10 MHz to 20 GHz. It is also shown that the proposed characterization methodology is able to detect any changes in material properties induced by changes in fabrication parameters such as sintering temperature. Ink conductivities of approximately 2.973×10^7 S/m and spacer dielectric constant of 1.78 were obtained for the inkjet printed CPWs on PET. In addition, the inkjet printed CPWs sintered at 170 °C and 220 °C on Kapton had conductivities of 0.187×10^7 and 0.201×10^7 S/m respectively. We verified our technique by measuring the material parameters with conventional approach.**

***Index Terms*—Inkjet printed CPW, flexible substrates, CAD, measurement, characterization.**

I. Introduction

TO ENABLE microwave circuits for emerging markets like the internet-of-things (IoT), there is a need for the inexpensive manufacture of environmentally friendly electronics. Thus, many traditional printing methods such as gravure printing, flexography, screen printing, and inkjet printing are making inroads into electronics manufacturing [1], [2]. Inkjet-printing has emerged as an alternative to conventional subtractive fabrication techniques such as etching and milling, since it is both cost-efficient and environmentally-friendly [3]. Unlike conventional etching and milling, where the waste includes hazardous chemicals, inkjet printing is an additive process, depositing controlled amounts of functionalized inks and producing no by-products [4]. Furthermore, inkjet printing is compatible with inexpensive flexible substrates such as polyethylene terephthalate (PET), photo paper, and Kapton. Numerous applications of inkjet printing have been reported for RF/microwave applications [5]-[7], including wireless power transfer topologies, RFID-based sensors [8], and microwave components [9]-[12] for low loss and high speed communication systems.

Measurement of electrical properties of inkjet printed components at RF/microwave frequencies elucidate fundamental properties of constituent materials including conducting inks and supporting dielectrics. Significant effort from the scientific community has been devoted to extract electrical properties of silver nanoparticle inks from these measurements. Some studies proposed extraction of propagation constant and characteristic impedance with the aid of complex scattering (S)-parameter measurements [13], [14]. K. Hettak *et al*. reported CPW on flexible PET with an attenuation of 0.6 dB/mm at 60 GHz [15]. Belhaz *et al*. showed a 0.3 dB/mm reduced losses at 67 GHz with a 300 °C sintering temperature [16]. Characterization based on conductivity analysis were presented in [17]-[19]. An adaptive, non-contact sensor measurement was proposed to extract the conductivity and current density in [20]. However, all of these approaches utilize analytical formulae to evaluate the ink conductivity, and require high precision microscopic measurements [21]. In addition, for repeatable measurements on flexible substrates, one has to address the most crucial challenges in flexible electronics such as performance distortion (substrate alignment) and delamination of integrated circuits (ICs) [22]. Computer-aided-design (CAD) based techniques utilizing commercial electromagnetic (EM) simulation packages are popular to extract dielectric properties from measured S-parameters [23], [24]. The problem with these techniques is that the simulation requires a prohibitive meshing or large number of iterations to find the dielectric constant that best matches the measured S-parameters.

Recently, we proposed a new approach to flexible printed electronics measurement as a first step toward developing a broadly-applicable test platform for evaluation of flexible, inkjet printed microwave circuits as well as their constituent materials [25]. Our approach enabled repeatable measurements for inkjet printed CPWs on a flexible PET substrate from 10 MHz to 20 GHz. In addition, we showed that with electromag-

A. Sahu and V. K. Devabhaktuni are with the Department of Electrical Engineering and Computer Science, The University of Toledo, Toledo, OH 43606 USA (e-mail: Abhishek.Sahu@utoledo.edu; Vijay.Devabhaktuni@utoledo.edu).

P. H. Aaen, G. P. Rigas and M. Shkunov are with Department of Electronic Engineering, Advanced Technology Institute, University of Surrey, UK (e-mail: p.aaen@surrey.ac.uk; g.p.rigas@surrey.ac.uk; m.shkunov@surrey.ac.uk).

A. Lewandowski is with Institute of Electronic Systems, Warsaw University of Technology, Warsaw, Poland (e-mail: A.Lewandowski@ise.pw.edu.pl).

T. M. Wallis and P. T. Blanchard are with the Electromagnetics division, NIST, Boulder, CO, USA, (e-mail: thomas.wallis@nist.gov; paulb@boulder.nist.gov)

netic simulation and optimization, it is possible to characterize the ink and supporting materials [26]. This paper develops and expands the main aspects of our previous work, and includes the following new significant additions:

1) A robust technique that reduces the computing resources and is able to obtain the values of the ink conductivity and spacer dielectric constant,
2) The technique automates all the subtasks involved in CAD modeling and optimization, thereby facilitating an efficient and concurrent parameter extraction framework,
3) Demonstration of the sensitivity of the CAD-assisted method to changes in fabrication, e.g. change in ink conductivity due to sintering temperature variation,
4) Extraction of capacitance per unit length and characteristic impedance for printed CPWs using a series resistor.

In Section II we present a detailed analysis to extract the microwave material parameters. We explain how to use the multiline TRL calibration and series resistor measurement to extract the propagation constant [27] and the characteristic impedance of the CPW [28]. We then present the interpolation-based EM modeling and least-square-based optimization process to fit the simulated attenuation and phase constant to measured values. We subsequently present a flow diagram that compares the proposed characterization approach with the conventional one to extract ink properties and dielectric constant of the spacer. In Section III, we present the fabrication and measurement methodology adopted for inkjet printed CPWs. In Section IV, the results from our proposed CAD-driven characterization technique are presented. The method is able to detect the changes in conductivity of the silver nanoparticle ink after sintering at different temperatures. Additionally, we present the simulated and measured attenuation constant, capacitance per unit length, characteristic impedance, and extracted ink conductivities and spacer dielectric constant. As will be shown, these results demonstrate a viable test platform for characterization of inkjet printed microwave circuits as well as the constituent materials. Finally, we conclude this paper in Section VI.

II. Characterization Methodology

An illustration of a CPW on a flexible substrate studied here is provided in Fig. 1. The desire to measure on-wafer CPWs with high precision leads to the need to support a wafer with minimal deformation while maximizing stiffness [29]. Flexible materials may be sensitive to mechanical probe contact during measurement. Vacuum chucks are suited to increase stiffness of these materials, however, the metallic vacuum chuck gives rise to a conductor-backed CPW (CBCPW), resulting in excitation of unwanted parallel-plate parasitic modes and microstrip modes.

We employed a dielectric spacer to avoid excitation of undesired modes. The spacer is planar and porous, thus ensuring uniform back support while distributing the vacuum equally throughout the surface and mitigating any potential deflection of the flexible substrate. The above topology can be easily analyzed as a multilayer CPW [30].

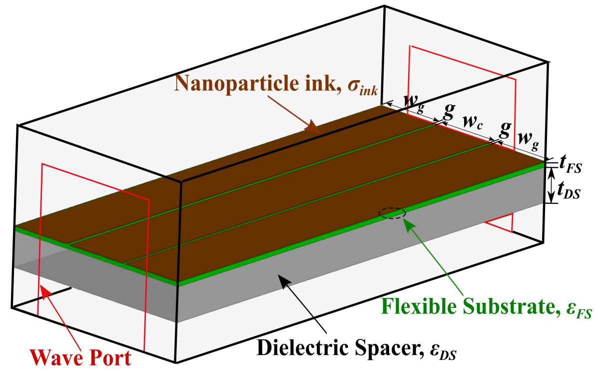

Fig. 1. Representative CPWs in a CAD environment. Silver nanoparticle inks of conductivity (σ_{ink}) are deposited on a (t_{FS}) thick flexible substrate to print CPWs with a ground plane of width (w_g), center conductor of width (w_c) and gap of width (g). During measurements, the CPWs are supported by a dielectric spacer of thickness (t_{DS}) underneath. ϵ_{FS} and ϵ_{DS} are dielectric constants of the flexible substrate and dielectric spacer respectively. CAD simulations are performed with waveguide port excitation.

A. Coplanar Waveguide Analysis

In this study, we used a multiline TRL calibration algorithm for determining the complex propagation constant from *uncalibrated* S-parameter measurements of multiple transmission lines [27]. In multiline TRL, the calibration is defined relative to the characteristic impedance of the transmission line (Z_0), which is complex and frequency dependent for normal metal transmission lines. For a series resistor, the assumption is that at low frequencies, the impedance (Z_L) can be approximated by the dc resistance of the resistor $Z_L \approx R_{DC}$. The dc resistance of the series resistor is determined experimentally from the difference between two-port dc measurements of the series resistor and the thru. Following the assumptions from [31], Z_0 for transmission lines on a low-loss substrate can be simplified as

$$Z_0 \approx \frac{\gamma(\omega)}{j\omega C_0}. \tag{1}$$

where $\gamma(\omega)$ is the frequency-dependent complex propagation constant obtained from the multiline TRL method and C_0 is capacitance per unit length of the CPW transmission lines.

The expression for the capacitance matrix, C obtained from a series resistor is [28]

$$C_{11,22} \approx \left(\frac{2\gamma(\omega)}{j\omega R_{DC}}\right)\frac{S_{11,22}}{1 - S_{11,22}} \tag{2}$$

$$C_{21,12} \approx \left(\frac{2\gamma(\omega)}{j\omega R_{DC}}\right)\frac{1 - S_{21,12}}{S_{21,12}}. \tag{3}$$

where S_{ij} denote S-parameters of the series resistor load. Once we obtain (2) and (3) from the reflection and transmission coefficients of a single series resistor, C_0 is then calculated by taking the average low-frequency limit of $C_{11,22}$ and $C_{21,12}$, thus providing estimates of C_0.

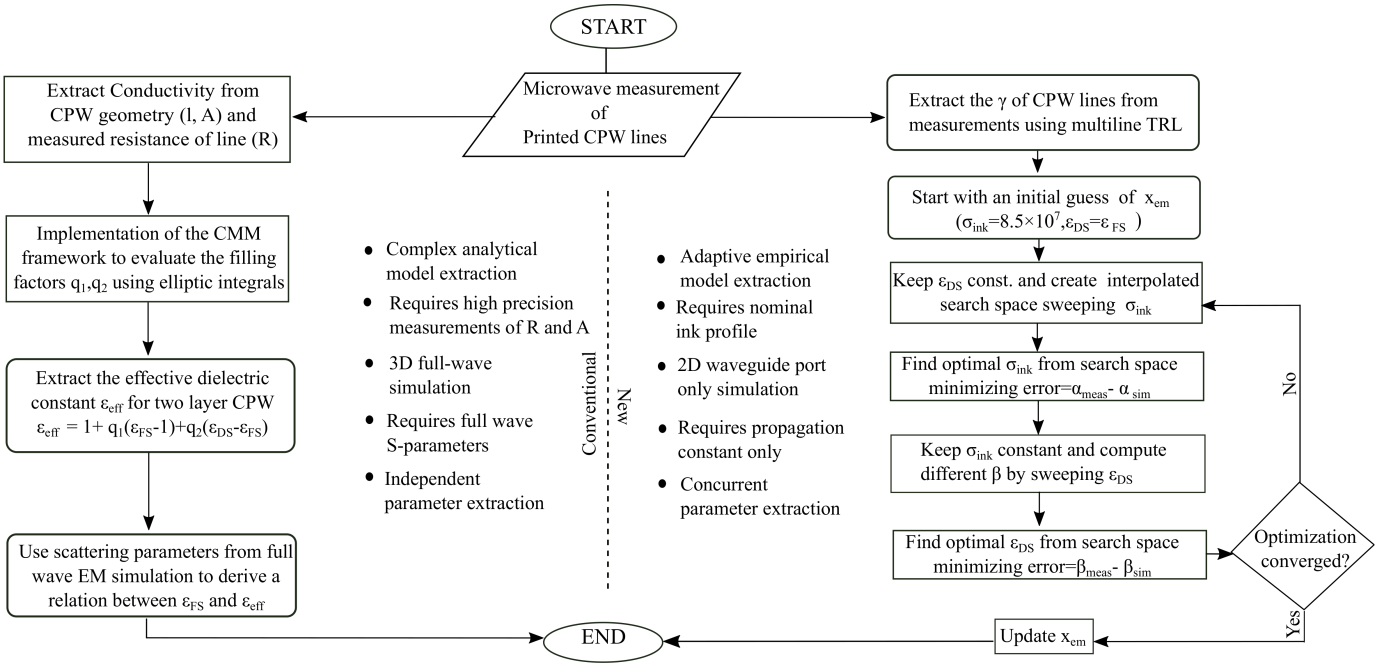

Fig. 2. Flow diagram of the conventional parameter extraction procedure with complex analytical CMM framework and full wave CAD simulation (left branch), against the proposed adaptive empirical model extraction with coarse meshed CAD simulation (right branch).

B. Modeling based Interpolation and Optimization

The multiline TRL calibration does not directly determine the material properties such as conductivity. Further, the effective dielectric constant (ϵ_{eff}) obtained from calibration is the weighted average of the different substrate dielectric constants in the multilayer CPW. Hence motivating use of EM simulation to extract the unknown substrate dielectric constant from ϵ_{eff}.

In the conventional approach, first the ϵ_{eff} is inferred from the scattering parameter measurements by means of a conformal mapping method (CMM) in combination with a parallel capacitance technique (PCT), which provides closed form formulas for ϵ_{eff} of the device [30]. However, CMM is based on quasi TEM propagation and requires multiple elliptical integrals to evaluate the filling factors. The second step involves deriving a relation between ϵ_{eff} and the unknown ϵ_{DS} utilizing full-wave EM simulated and measured S-parameters. As this analytical framework requires calculation of multiple complex elliptical integrals and fine meshed full-wave simulated S-parameters, it can be cumbersome, time consuming and requires significant computational resources.

The inherent challenges of this conventional parameter extraction technique is further augmented by the need to make additional high precision microscopic and resistance measurements to obtain conductivity. The dc conductivity of the inkjet printed silver nanoparticles is generally extracted using the measured profiles of the printed traces following [5]

$$\sigma_{ink}^{dc} = \frac{l}{R \cdot A}. \tag{4}$$

where σ_{ink}^{dc} is dc conductivity (S/m), l is the length of the CPW, R is the CPW measured resistance (Ω) and A is the cross sectional area of the CPW. The cross section areas of printed traces may be determined by accurate profilometry and numerically integrating over the number of printed layers. An in-depth discussion on challenges of conventional conductivity measurement techniques has been reported in [21].

In order to overcome the above problems, we propose an alternative CAD-based extraction technique. Here, we first developed an EM-simulated, finite-element model to map the microwave properties of the CPW lines (attenuation constant α, phase constant β) relative to unknown material properties ($\sigma_{ink}, \epsilon_{DS}$) and frequency ($\omega$). The output parameter Y and unknown material properties for the model x are represented as

$$x = \begin{bmatrix} \sigma_{ink} \\ \epsilon_{DS} \end{bmatrix}, Y = \begin{bmatrix} \alpha \\ \beta \end{bmatrix}. \tag{5}$$

where attenuation and phase constants of the CPW lines can be obtained from the simulated propagation constant γ using the classical relationship

$$\gamma = \alpha + j\beta. \tag{6}$$

Once the finite element model is developed, a search space is then created dynamically which offers interpolated values of Y at specific query points for x and ω. Subsequently, x can be obtained through a non-linear optimization in the search space, thus minimizing the deviation between the models and measurements. The interpolated matrices can be represented as $Y_{em}(x_{em}, \omega)$. Whereas, the measurement in this case, has a response represented by $Y_m(x_m, \omega)$. In general, these models are defined in two parameter spaces x_m and x_{em}. The goal is to perform minimum number of EM simulations in finding a non-linear least square solution x^*_{em} with $Y_{em}(x^*_{em}, \omega)$ as close to $Y_m(x_m, \omega)$ as possible, where,

$$x^*_{em} = arg\{min(\sum_{\omega} ||Y_m(x_m, \omega) - Y_{em}(x_{em}, \omega)||)\}. \quad (7)$$

We optimized the values of both material parameters of interest by solving this non-linear least square problem, following Levenberg-Marquardt algorithm, which helps to avoid the local minima. The lower and upper bounds for the optimization algorithm for each iteration were set as the minimum and maximum value of σ_{ink} and ϵ_{DS} from EM simulation.

C. Parameter Extraction

A flow diagram depicting the proposed parameter extraction procedure is shown in Fig. 2. The first step of the procedure consists of extracting the propagation constant of the CPW lines directly from measurements using multiline TRL calibration. Next, an EM analysis with an initial guess of x is performed. To consider a uniform, two-layer CPW structure, we defined σ_{ink}= 8.5×10^7 S/m (equal to copper) and ϵ_{DS}=ϵ_{FS} as the initial guess of x. As regarding the other material parameters, such as the loss tangent (tan δ) and ϵ_{FS} of the flexible substrates, final values were adopted from the literature but the process we developed could be expanded to include these as well. Next, a search space is created by sweeping the σ_{ink}, while keeping ϵ_{DS} constant. Following (7), we then extracted the optimal value of σ_{ink} by minimizing the difference between modeled and measured attenuation constant (summed over all frequencies) using a least-square algorithm.

The design parameter x is then updated with the new σ_{ink}. In the next iteration, the search space is created with ϵ_{DS} sweep, while keeping the σ_{ink} constant and phase constant from measurement and simulation is considered as the optimization criteria. The above steps are iterated till we attain a least square error $\approx 1\times10^{-4}$ and finally the design parameter x provides the values for unknowns σ_{ink} and ϵ_{DS}.

In this work, the whole procedure was automated and controlling software (MATLAB^{TM}) was interfaced with the EM simulator *Ansys HFSS*$^{TM\|}$, enabling a robust platform to extract the unknown parameters. Our interpolation and error minimization tasks are based on the Optimization Toolbox in Matlab [32].

Contrary to the classical approach, the proposed technique concurrently determines all of the necessary material parameters utilizing only a single set of calibrated S-parameter measurements. These parameters that can be readily used in the electromagnetic simulator to enable accurate simulations of more complex circuits. Furthermore, as the optimization objective function requires just the propagation constant, a two-dimensional finite element simulation for waveguide port excitation solutions of the CPW cross section would suffice. In this way, the total time and computing resources is expected to diminish very quickly with an increasing search space of design parameter x.

‖Trade names are used for clarity and do not imply endorsement by NIST.

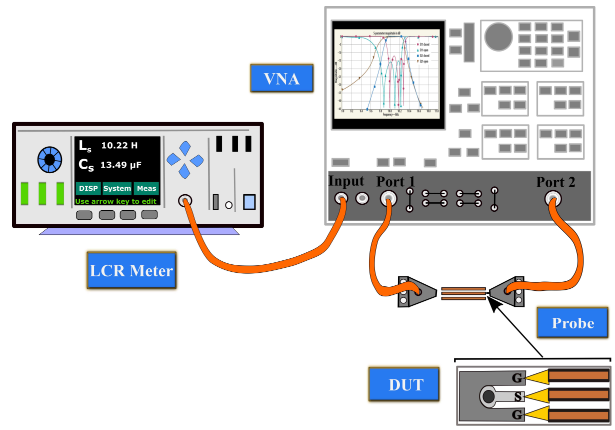

Fig. 3. Schematic of the measurement setup. A LCR meter is connected to the VNA to measure the dc resistance of THRU and series resistor.

III. Fabrication and Measurement

A. Fabrication

To demonstrate that the proposed technique is applicable to multiple processing parameters, we fabricated two sets of printed CPW lines with different printing methods. In the first set, the printing was carried out using a commercial process with Inkjetflex [33]. This process uses inkjet printing as a precursor on which copper is electroplated. This overcomes the low resistance issues that commonly occur with traditional nanoparticle inks used in inkjet processes. The process uses reel-to-reel printing. The printing was performed at 360 dots per inch in a single printing pass. The prototyping for the circuit was performed using a sheet resistance of 30 mΩ/mm^2. The CPW lines (Fig. 1) have a 1.983 mm center conductor (w_c), a 0.130 mm gap (g), and 1.983 mm wide ground planes (w_g) fabricated on 125-μm-thick (t_{FS}) PET substrate with approximately 2 μm copper plating. To complete a benchmark multiline TRL calibration, the fabrication included a set of 6 CPWs with lengths of l=(14.97 mm, 18.42 mm, 23.57 mm, 35.78 mm, 61.60 mm, 97.93 mm), a symmetric short circuit and a reflect standard. The reflect standard consisted of a 6.50-mm-long transmission line on each port centered about the termination. The lengths were determined based on the approach in [34].

The second set of CPW devices with similar dimensions were fabricated using a drop-on-demand Dimatrix DMP-2800 inkjet printer. Custom-modified nanoparticle ink (Aldrich) with 150 nm particle size was printed as a single layer to define the patterns. In addition to the change in printing technique, we modified other variables to validate the robustness of the proposed approach. In the second set of devices, instead of PET a 125-μm-thick Kapton was used as a substrate and different sintering temperature were introduced to obtain Ag tracks with different conductivities. Two sets of CPWs were fabricated with sintering temperature of 170 °C and 220 °C. As before, to complete a benchmark multiline TRL calibration, the fabrication included a set of 5 CPWs with lengths of l=(6.00 mm, 8.33 mm, 12.99 mm, 17.65 mm, 19.98 mm), a 6.50-mm-long symmetric short circuit reflect standard and a

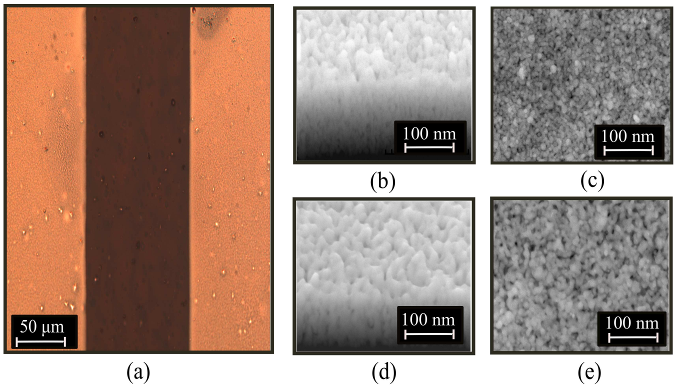

Fig. 4. (a) Zoomed microphotograph of printed CPW lines on Kapton. (b) Tilt-view SEM images of a cross-section of the ink layer sintered at 170 °C. (c) SEM Image showing granular ink particles sintered at 170 °C. (d) Tilt-view SEM images of a cross-section of the ink layer sintered at 220 °C. (e) SEM Image showing granular ink particles sintered at 220 °C.

series resistor standard. For the series resistor, a 50 Ω surface mount resistor was adhered to the center trace of the CPW using a silver conductive epoxy.

B. Measurement

Fig. 3 depicts a schematic of the measurement setup. Two-port S-parameter measurements were carried out with a vector network analyzer (VNA) and an on-wafer measurement platform. The system includes two ground-signal-ground (GSG) microwave probes (1.0 mm pitch), probe manipulators, and an optical microscope. As described before, during measurements, the flexible substrate was supported by a 0.5 cm-thick (t_{DS}) porous, dielectric. The power level of VNA was set to -17.0 dBm and the uncorrected S-parameters were measured for each device from 10 MHz to 20 GHz. A LCR meter was connected with the VNA to measure the dc resistance of the THRU. In order to test the repeatability, four sets of measurements were carried out at two separate laboratories on nominally identical sets of devices. An optical image of an inkjet-printed CPW device is shown in Fig. 4(a). Scanning electron microscope (SEM) images of CPW devices sintered at 170 °C are shown in Figs. 4(b) and 4(c), while SEM images of CPW devices sintered at and 220 °C are shown in Figs. 4(d) and 4(e). Inspection of the respective SEM images of the devices sintered at 170 °C and 220 °C reveals an increased grain size at the higher sintering temperature, which is consistent with previous results [16]. The root-mean-square (rms) surface surface roughness of the inkjet-printed devices on Kapton was measured by use of an optical profilometer.

IV. Results and Analysis

Here, we present results obtained for parameter extraction of inkjet printed CPW lines on different flexible substrates with various processing parameters. We divide the results into two sections: 1) Multiline TRL Analysis 2) Parameter Extraction outputs.

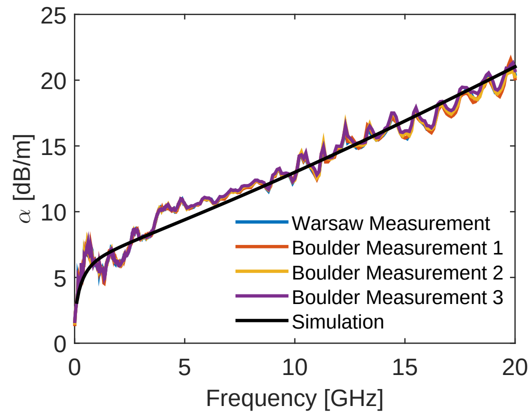

Fig. 5. Attenuation constant obtained from four sets of repeatable measurements on PET and EM simulation. The red line, yellow line and purple line represent the attenuation constants from Boulder measurements and the blue line represent the measurement from Warsaw. The black line shows the attenuation constant from *HFSS* simulation.

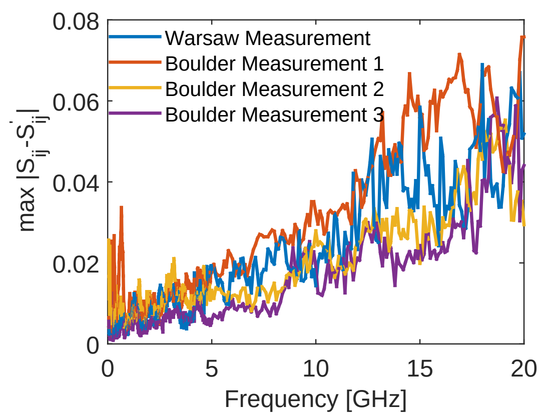

Fig. 6. Maximum deviation in S-parameters between four sets of successive mutiline TRL calibrations on PET are shown. The red, blue, yellow and purple curves (in online version) show the maximum difference between calibration coefficients from four sets of measurements at two labs.

A. Multiline TRL Analysis

Fig. 5 shows the attenuation constant as a function of frequency for inkjet printed CPW lines on PET. It can be seen that loss increases with frequency. As measured propagation constant and multiline TRL calibration are the most crucial components of our technique, we verified the measurement repeatability through four sets of measurements; each with a pre- and post-calibration. As can be seen in Fig. 5, the four sets of measurements agree quite well with each other, confirming the attenuation constant repeatability. Fig. 6 shows a comparison of calibration coefficients for the four sets of measurements following the technique presented in [35]. This technique evaluates the worst-case deviations of the measured S-parameters for an examined calibration with respect to a benchmark calibration. Deviations are treated as $\max(|S_{ij} - S_{ij'}|)$ for ij ∈ 11, 12, 21, 22, where $S_{ij'}$ is the S-parameter measured by the first (or pre) calibration to be tested, and S_{ij} is the S-parameter measured by the second (or post) calibration.

The worst-case difference demonstrates the repeatability of multiline TRL calibrations.

One of the primary objectives of this research is to show that the proposed technique is able to detect changes in fabrication parameters. Here, we adopt sintering temperature as the case study [16], [19]. We first studied the influence of the sintering temperature on attenuation. Specifically, we characterized lines sintered at 170 °C and 220 °C for 30 min each. Fig. 7 shows the attenuation constant versus frequency for the two different heating temperatures 170 °C and 220 °C. One can see that losses decrease by about (40 dB/m) at 20 GHz when we change the sintering temperature from 170 °C to 220 °C, reflecting the decrease of the resistivity. To confirm the difference in attenuation constant, we performed repeatable measurements for both samples over a period of several weeks. In Fig. 7 the dashed lines with crosses represent attenuation constants from repeated measurements. The two sets of measurements for both samples agree quite well with each other, confirming change in attenuation constant due to variation in sintering temperature.

We then used (2)-(3) for the series resistor to evaluate C_0 with $\gamma(\omega)$ determined by the multiline TRL algorithm. In Fig. 8, the capacitance per unit length C extracted from (2), using the reflection coefficient data for series resistor, is shown as the solid red and blue lines; the corresponding value calculated from (3) using the transmission coefficient data, is shown as the solid green and black lines (in online version). Fig. 8 shows that below 1 GHz, C obtained from reflection and transmission data is between 0.6 pF/cm to 0.8 pF/cm. We then used the mean value below 1 GHz to estimate C_0 at zero frequency and obtain a value of 0.7 pF/cm. This value is consistent with the capacitance per unit length obtained from finite element simulations of the cross-sectional CPW geometry on Kapton. We then obtained the characteristic impedance of the CPW lines from equation (1). Fig. 9 displays Z_0 computed from γ and C_0 for both sets of inkjet printed CPWs on Kapton. The results are in good agreement with the designed characteristic impedance.

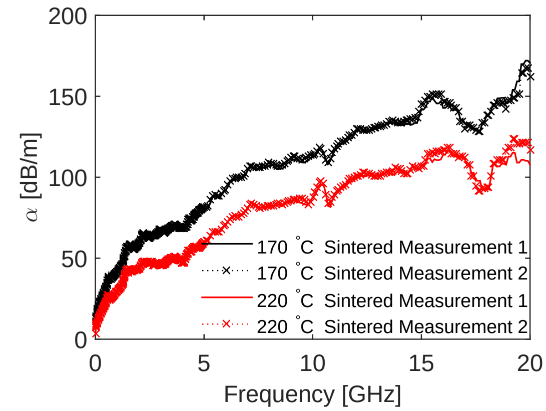

Fig. 7. Attenuation constants obtained from two sets of printed components on Kapton with different sintering temperature. The black line and red lines (in online version) represent the attenuation constants from Boulder measurements for printed CPW lines sintered at 170 ^{0}C and 220 ^{0}C. The dashed lines with crosses depict the repeated measurements for both sintered samples.

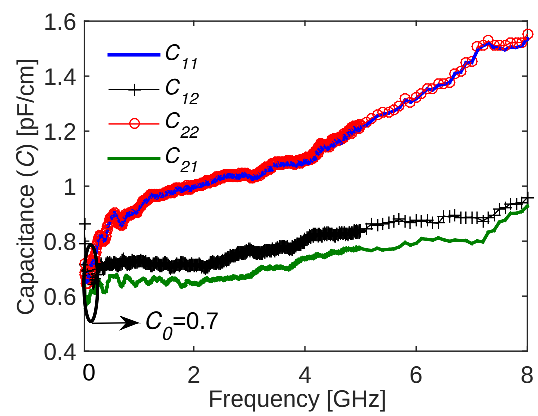

Fig. 8. Capacitance per unit length extracted from the series resistor standard on Kapton. The red and blue curves show the C_{11} and C_{22} respectively, extracted from the series resistor reflection coefficients of the corrected S-Parameters and the blue and black lines show the C_{12} and C_{21} respectively, from the transmission coefficients. C_0 is determined by taking the average low-frequency limit of all curves.

B. Parameter Extraction

Following the methodology described in section II, we performed several iterations to estimate the value of σ_{ink} and ϵ_{DS}. To further simplify the procedure, reduce time and memory consumption, we interpolated the measurement data utilizing the EM simulation grid. This resulted in a much smaller data set to carry out the modeling. We first demonstrate the technique on inkjet printed CPWs on PET. The dielectric constant and loss tangent of PET substrate were defined as 3.1 and 0.01. Additionally, the initial values for σ_{ink} and ϵ_{DS} were set as 8.54×10^7 S/m (same as copper) and 3.1 (same as PET) to define a uniform model to initiate the optimization routine. After each iteration, the automated search updates the search range by observing the results from previous iterations. A 2-D interpolated search space was created dynamically between the simulated CPW response and material parameters as described in section II-B. It was observed that the least square optimization routine converged after 7 iterations with an aggregated error of 4×10^{-4}. The final values of σ_{ink} and ϵ_{DS} of the dielectric spacer were found to be 2.973×10^7 S/m and 1.78. Fig. 5 depicts the comparison of attenuation constant from EM simulation with extracted parameters and measurement. The normalized phase constant can be calculated by dividing β by the free space phase constant, $\beta_0 = 2\pi f/c$, where c is the speed of the light. A comparison plot for normalized phase constant from measurement and simulation is shown in Fig. 10. As can be observed, both the plots are in agreement, thus demonstrating the effectiveness of the proposed methodology. Furthermore, it was also observed that the losses in the CPW lines are mostly affected by the conductivity of the ink and loss tangent of PET substrate. The loss tangent of the dielectric spacer is very low and has minimal effect on the overall losses of the CPW lines.

CAD-based modeling and characterization techniques are known to be sensitive to the design variables [36]. In order

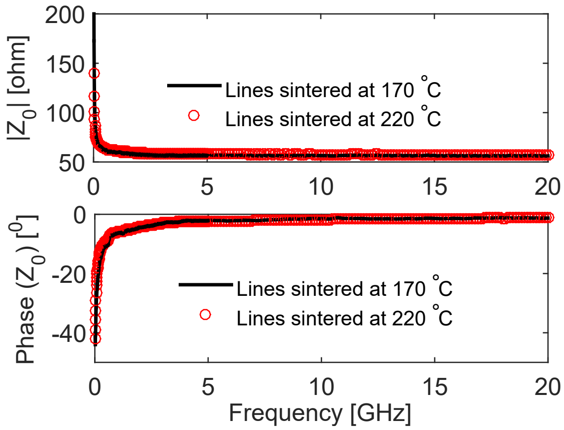

Fig. 9. Characteristic impedance of CPW lines on Kapton. Upper and lower curves plot magnitude and phase of (Z_0), respectively, based on the measurement of γ and C_0 from series resistor standard. The red and black lines (online version) represent capacitance per unit length from 170 ^{0}C and 220 ^{0}C sintered samples, respectively.

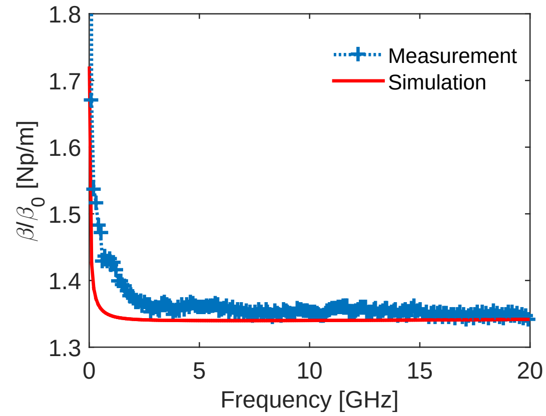

Fig. 10. Comparison of normalized phase constant from the inkjet printed CPW lines on Kapton. The normalization is achieved by diving the phase constant with free space phase constant, $\beta_0 = 2\pi f/c$, where c is the speed of the light. The red curve denotes the normalized phase constant from simulation and dashed blue curve (in online version) depicts from measurement.

TABLE I
EXTRACTED CONDUCTIVITY AND SPACER DIELECTRIC CONSTANT FOR INKJET PRINTED CPWS ON DIFFERENT FLEXIBLE SUBSTRATES

Test Samples	$\sigma_{ink}(10^7$S/m)	ϵ_{DS} (Sim.)	ϵ_{DS} (Meas.)
PET	2.973	1.78	1.81
Kapton 170 °C	0.187	1.76	1.79
Kapton 220 °C	0.201	1.81	1.84

TABLE II
COMPARISON OF SIMULATED AND MEASURED CONDUCTIVITIES

Test Samples	$R_{DC}(\Omega)$	$\sigma_{ink}^{sim}(10^7 S/m)$	$\sigma_{ink}^{meas}(10^7 S/m)$
170 °C	3.65	0.187	0.192
220 °C	2.95	0.201	0.206

to quantify the applicability of the proposed characterization methodology to detect change in sintering temperature, we repeated the analysis described in this section for measurements at different temperatures: 170 ^{0}C and 220 ^{0}C. In this instance, the dielectric constant and loss tangent of Kapton were defined as 3.4 and 0.1 [17] in the *HFSS* model. Like the previous scenario, the initial values for σ_{ink} and ϵ_{DS} were set as 8.54×10^7 S/m (same as copper) and 3.4 (same as Kapton) to define an uniform model for iteration 1. The final values of σ_{ink} for 170 °C and 220 °C were found to be 0.187×10^7 S/m and 0.201×10^7 S/m respectively. Table I reports, the extracted σ_{ink} and ϵ_{DS} for printed CPWs.

In order to further verify if the extracted material properties are correct, σ_{ink} and ϵ_{DS} were determined using alternative approaches. First, the spacer dielectric constant ϵ_{DS} was measured at Boulder and Warsaw utilizing macroscopic measurement techniques. For the frequency region below 5 GHz, a split post resonator method [37] was adopted at Warsaw to measure the ϵ_{DS}. The resulted ϵ_{DS} was noted to be 1.81. Further, for frequency between 18 GHz and 27 GHz, we employed a waveguide technique at Boulder to measure ϵ_{DS} employing a WR42 waveguide [38]. The measured ϵ_{DS} was noted to be between 1.79 and 1.84 and reported in Table I. Measurements from both techniques confirm that the value is constant with frequency, as expected over the measured frequency range.

As an additional verification, dc conductivity for the printed CPW lines were measured. Equation (4) is widely cited in the literature as an accurate calculation of dc conductivity for inkjet printed transmission lines [17]. Following the same technique, we measured the dc resistance of printed CPW lines using a LCR meter connected to the VNA as depicted in Fig. 3. The resistance of the THRU lines for both samples were measured to be 3.65 Ω and 2.95 Ω, respectively. Table II reports a comparison of measured dc conductivity and extracted conductivity by our approach. As can be seen, we are able to verify values of material parameters using a nominal ink profile in the EM simulation. This suggests that our procedure may be of use in areas where the process leads to a predictable or well-known profile, e.g. manufacturing processes.

Last but not least, the effect of surface roughness was investigated. The rms roughness of the devices sintered at 170 °C was 80 ± 13 nm while the rms roughness of the devices sintered at 220 °C was 86 ± 13 nm. It is very small compared to the skin-depth of Ag at 20 GHz and hence was ignored in the EM simulation. However, note that, for frequencies above 50 GHz, where the rms surface roughness is comparable to skin-depth, surface roughness must be incorporated into the finite element model.

V. ACKNOWLEDGMENT

The authors thank the critical review of Dr. J. Booth, Dr. N. D. Orloff, and Dr. C. J. Long, all with the National Institute of Standards and Technology (NIST), for their critical feedback during the course of this research, and their comments on this papers manuscript.

VI. Conclusion

This paper proposes a robust methodology for microwave characterization of CPW lines on flexible substrates such as PET and Kapton. First, metrology based on on-wafer TRL was proposed to measure the printed samples on a flexible substrate which avoids unnecessary parasitic modes for CPWs. A detailed measurement-based CPW analysis was carried out to extract the microwave parameters such as propagation constant, capacitance per unit length and characteristic impedance. Further, using a CAD based technique, we were able to extract the ink conductivity and dielectric constant of the spacer used for measurement. Employment of CAD enabled full automation of the extraction procedure. It was demonstrated that the resulting robust characterization methodology is able to detect the variation in fabrication parameters such as sintering temperature. The extracted conductivity of the ink and spacer dielectric constant were found to be in good agreement with the measured values. Direct measurement of the device profile may be useful to reduce uncertainty in the extracted parameters, but a nominal profile is sufficient to extract a physically reasonable (and in this case, verified) value. In design applications, a short extraction time and straightforward extraction procedure make the CAD model a good replacement for the time-consuming and experience-demanding analytical procedure of traditional approach.

References

[1] Y. Kim, H. Kim and H.-J. Yoo, "Electrical Characterization of Screen-Printed Circuits on the Fabric," *IEEE Trans. Adv. Pack.*, vol. 33, no. 1, pp. 196205, Feb. 2010.

[2] R. Vyas, V. Lakafosis, H. Lee, et al., "Inkjet printed, self -powered, wireless sensors for environmental, gas, and authentication-based sensing," *IEEE Sens. J.*, vol. 11, no. 12, pp. 3139-3152, Dec. 2011.

[3] L. Yang, A. Rida, R. Vyas, M. M. Tentzeris, "RFID tag and RF structures on a paper substrate using inkjet-printing technology," *IEEE Trans. Microw. Theory Techn.*, vol. 55, no. 12, pp. 2894-2901, Dec. 2007.

[4] M. A. Ziai and J. C. Batchelor, "Temporary on-skin passive UHF RFID transfer tag," *IEEE Trans. Antennas Propag.*, vol. 59, no. 10, pp. 3565-3571, Oct. 2011.

[5] S. Kim et al., "Inkjet printed antennas, sensors and circuits on paper substrate," *IET Microw. Antennas Propag.*, vol. 7, no. 10, pp. 858-868, Jul. 2013.

[6] G. A. Casula, G. Montisci and G. Mazzarella, "A Wideband PET InkjetPrinted Antenna for UHF RFID," *IEEE Antennas Wireless Propag. Lett.*, vol. 12, pp. 1400-1403, 2013.

[7] L. Xiang, Z. Wang, Z. Liu, S. E. Weigum, Q. Yu and M. Y. Shen, "Inkjet-Printed Flexible Biosensor Based on Graphene Field Effect Transistor," *IEEE Sensors J.*, vol. 16, no. 3, pp. 8359-8364, Dec. 2016.

[8] S. Kim, A. Georgiadis, A. Collado, and M. M. Tentzeris, "An inkjet-printed solar-powered wireless beacon on paper for identification and wireless power transmission applications," *IEEE Trans. Microw. Theory Techn.*, vol. 60, no. 12, pp. 4178-4186, Dec. 2012.

[9] S. Kim et al., "Fabrication of fully inkjet-printed vias and SIW structures on thick polymer substrates," *IEEE Trans. Compon. Manuf. Pack.*, vol. 6, no. 3, pp. 486-496, Mar. 2016.

[10] T. Peter, Y. Y. Sun, T. I. Yuk, H. F. AbuTarboush, R. Nilavalan and S. W. Cheung, "Miniature transparent UWB antenna with tunable notch for green wireless applications," *Antenna Technology (iWAT)*, 2011 International Workshop on, pp. 259-262.

[11] K. Hettak et al, "Low-cost mm-wave coplanar waveguide bandpass filter using inkjet printing of silver nano-particles on flexible plastic substrate," *Proc. IEEE International Microwave Symposium*, 17-22 May 2015, pp: 1-3.

[12] A. Manicanin, L. Zivanov, C. Zlebic, M. Kisic, N. Blaz and M. damnzanovic, "Fully inkjet printed CPW meander inductors on PET flexible substrate," *in 38th Int. Spring Seminar on Elect. Tech.*, Eger, May 6-10 2015, pp. 43-46.

[13] B. Shao, R. Weerasekera, L. R. Zheng, R. Liu, W. Zapka and P. Lindberg, "High Frequency Characterization of Inkjet Printed Coplanar Waveguides," *12th IEEE Workshop on Signal Propagation on Interconnects*, Avignon, 2008, pp. 1-4.

[14] P. Xu and M. C. Hamilton, "Reduced-Loss Ink-Jet Printed Flexible CPW With Copper Coating," *IEEE Microw. Wirel. Compon. Lett.*, vol. 23, no. 4, pp. 178-180, April 2013.

[15] K. Hettak, T. Ross, R. James, A. Momciu and J. Wight, "Flexible Polyethylene Terephthalate-based inkjet printed CPW-fed monopole antenna for 60 GHz ISM applications," *Microwave Conference (EuMC), 2013 European*, pp. 1447-1450.

[16] M. M. Belhaj, W. Wei, E. Pallecchi, C. Mismer, I. Roch-jeune and H. Happy, "Inkjet printed flexible transmission lines for high frequency applications up to 67 GHz," *European Microw. Integ. Cir. Conf. (EuMIC)*, 2014 9th, Rome, 2014, pp. 584-587.

[17] S. Swaisaenyakorn, P. R. Young and M. Shkunov, "Characterization of ink-jet printed CPW on Kapton substrates at 60 GHz" *Loughborough Antennas and Propagation Conference (LAPC)*, 2014, UK, pp. 676-678.

[18] C. Paragua, K. Frigui, S. Bila and D. Baillargeat, "Study and characterization of CNT Inkjet printed patterns for paper-based RF components," *2015 European Microwave Conference (EuMC)*, paris, 2015, pp. 861-864.

[19] J. Niittynen and M. Mntysalo, "Characterization of Laser Sintering of Copper Nanoparticle Ink by FEM and Experimental Testing," *IEEE Trans. Compon. Pack. Manuf. Tech.*, vol. 4, no. 12, pp. 2018-2025, Dec. 2014.

[20] C. Beisteiner, R. Wallner and B. G. Zagar, "Electrical characterization of inkjet printed conductive traces using LinuxCNC," *2015 IEEE Int. Instrum. Meas. Tech. Conf. (I2MTC) Proceedings*, Pisa, 2015, pp. 1883-1888.

[21] C. Wargo, "Characterization of conductors for printed electronics," Technical report, PChem Associates, Bensalem, PA.

[22] A. Traille, S. Kim, A. Coustou, H. Aubert and M. M. Tentzeris, "A conformal/rollable monolithic miniaturized ultra-portable ground penetrating radar using additive and inkjet printing," *2014 IEEE MTT-S Int. Microw. Symp. (IMS2014)*, Tampa, FL, 2014, pp. 1-4.

[23] Hong-Duc Nguyen et al., "RF characterization of flexible substrates for new conformable antenna systems," *2016 10th European Conf. Ant. Propag. (EuCAP)*, Davos, 2016, pp. 1-5.

[24] Z. Yang, A. Takacs, S. Charlot and D. Dragomirescu, "Design of Kapton based passive circuits at microwave frequencies," *2015 European Microw. Conf. (EuMC)*, Paris, 2015, pp. 873-876.

[25] A. Sahu, V. Devabhaktuni, A. Lewandowski, P. Barmuta, T. M. Wallis, M. Shkunov and P. Aaen, "Microwave Characterization of Ink-Jet Printed CPW on PET Substrates," *in 86th ARFTG Microwave Measurment conference.*, Atlanta, GA, Dec. 3-4 2015, pp. 1-4.

[26] A. Sahu, V. Devabhaktuni, A. Lewandowski, T. M. Wallis, P. Aaen, "CAD-Assited microwave characterization of Ink-Jet printed CPW on PET substrates," *in 88th ARFTG Microwave Measurment conference.*, Austin, TX, Dec. 6-9 2016, pp. 1-4.

[27] R. B. Marks, "A multiline method of network analyzer calibration," *IEEE Trans. Microw. Theory Tech.*, vol. 39, no. 7, pp. 1205-1215, Jul. 1991.

[28] N. D. Orloff *et al.*, "A Compact Variable-Temperature Broadband Series-Resistor Calibration," *IEEE Trans. Microw. Theory Tech.*, vol. 59, no. 1, pp. 188-195, Jan. 2011.

[29] C. Gaal and J. Sinha "Ring chuck to hold 200 and 300 mm wafer," U.S. Patent 6538733 B2, Mar., 25, 2003.

[30] M. Ouaddari, S. Delprat, F. Vidal, M. Chaker and Ke Wu, "Microwave characterization of ferroelectric thin-film materials," *IEEE Trans. Microw. Theory Techn.*, vol. 53, no. 4, pp. 1390-1397, April 2005.

[31] R. B. Marks and D. F. Williams, "Characteristic impedance determination using propagation constant measurement," *IEEE Microw. Guided Wave Lett.*, vol. 1, no. 6, pp. 141-143, June 1991.

[32] T. P. Crummey, R. Farshadnia, P. J. Fleming, A. C. W. Grace and S. D. Hancock, "An optimization toolbox for MATLAB," *Int. Conf.Control 1991.*, Edinburgh, 1991, pp. 744-749 vol.2.

[33] http://inkjetflex.com/site/rapid-prototyping/.

[34] A. Lewandowski, W. Wiatr, L. J. Opalski, R. Biedrzycki, "Accuracy and bandwidth optimization of the over-determined offset-short reflectometer calibration" *IEEE Trans. Microw. Theory Tech.*, vol. 63, no. 3, pp. 1076-1089, March 2015.

[35] D. F. Williams and R. B. Marks, "Comparison of on-wafer calibrations," *in 38th ARFTG Cong. Dig.*, San Diego, CA, Mar. 1992, pp. 68-81.

[36] J. C. Booth, N. D. Orloff, J. Mateu, M. Janezic, M. Rinehart, and J. A. Beall, "Quantitative permittivity measurements of nanoliter liquid volumes in microfluidic channels to 40 GHz," *IEEE Trans. Instrum. Meas.*, vol. 59, no. 12, pp. 3279-3288, Dec. 2010.

[37] J. Krupka, W. Gwarek, N. Kwietniewski and J. G. Hartnett, "Measurements of Planar MetalDielectric Structures Using Split-Post Dielectric Resonators," *IEEE Trans. Microw. Theory Techn.*, vol. 58, no. 12, pp. 3511-3518, Dec. 2010.
[38] T. Chiu, "Dielectric constant measurement technique for a dielectric strip using a rectangular waveguide," *IEEE Trans. Instrum. Meas.*, vol. 52, no. 5, pp. 1501-1508, Oct. 2003.

Abhishek Sahu (S'13) was born in India in 1990.He received the B.Tech degree in ECE from BPUT, India, in 2012. In 2013, he joined the EECS Department at the University of Toledo, where is currently working towards his Ph.D. degree in electrical engineering. His present research interests are applied electromagnetics, mm-wave components design and microwave measurement techniques. Mr. Sahu is the recipient of the Best Student Paper Award at the Applied Electromagnetic Conference, India, 2011 and ARFTG Microwave symposium, Atlanta, 2015.

Peter H. Aaen (S'93-M'97-SM'09) received the B.A.Sc. degree in Engineering Science and the M.A.Sc. degree in Electrical Engineering, both from the University of Toronto, Toronto, ON., Canada, and the Ph.D. degree in Electrical Engineering from Arizona State University, Tempe, AZ., USA, in 1995, 1997 and 2005, respectively. He joined the Faculty of Engineering and Physical Sciences at the University of Surrey in 2013, where he is a Reader in Microwave Semiconductor Device Modeling. Before joining the University of Surrey, he was the Manager of the RF Modeling and Measurement Technology team of the RF Division of Freescale Semiconductor, Inc, Tempe, AZ, USA; a company which he joined in 1997 (then Motorola Inc. Semiconductor Product Sector).

His areas of expertise include calibration techniques for microwave measurements, development of package modeling techniques, development of passive and active compact models for the design of microwave power transistors and ICs, and efficient electromagnetic simulation and optimization methodologies for complex packaged environments. Dr. Aaen is a Senior Member of the IEEE, a member of the Microwave Theory and Techniques Society, and is an active member of many technical committees including: MTT-1 Computer-Aided Design, technical program committee (TPC) of the IEEE Conference on Electrical Performance of Electronic Packaging and Systems, and the IMS TPRC sub-committee for CAD Algorithms and Techniques. Most recently he served the ARFTG community as the Technical Program Chair for the 78th and 82nd Symposiums and is the e-Publicity chair for the ARFTG Executive Committee. He co-authored Modeling and Characterization of RF and Microwave Power FETs (Cambridge University Press, 2007) and has authored over forty papers, articles and workshops in the fields of electromagnetic simulation, package modeling, and microwave device modeling and characterization.

Arkadiusz Lewandowski (M'09) received the M.Sc. degree and the Ph.D degree (hons.) in electrical engineering from the Warsaw University of Technology, Warsaw, Poland, in 2001 and 2010, respectively. He joined the Institute of Electronics Systems, Warsaw University of Technology, in 2002, where he conducts research in the area of microwave measurements. From 2002 to 2004 he was involved in the development of digital synthesizers of radar signals with the Telecommunications Research Institute, Warsaw, Poland. From 2004 to 2008 he was a Guest Researcher at the National Institute of Standards and Technology, Boulder, CO, USA, where was engaged in the development of uncertainty analysis and calibration methods for coaxial and on-wafer VNA measurements. His current research interests concern small- and large-signal microwave measurements, and modeling of passive and active microwave devices. Dr. Lewandowski was the recipient of Best Paper Award at the International Microwave Conference MIKON 2008, Poland and the 2005 MTT-S Graduate Fellowship Award.

T. Mitch Wallis (S'97-M'03-SM'09) received the B.S. degree in physics from the Georgia Institute of Technology, Atlanta, in 1996, and the M.S. and Ph.D. degrees in physics from Cornell University, New York, in 2000 and 2003, respectively. Since 2003, he has been at the National Institute of Standards and Technology, Boulder, CO. He was a National Research Council Postdoctoral Fellow from 2003 to 2005 and is currently a Staff Physicist. His research interests include development of high-frequency scanning probe microscopes and other metrology for high-speed nanoscale electronics and spintronics.

Maxim Shkunov (M'10) studied physics and applied mathematics at Moscow Institute of Physics and Technology (diploma/M.Sc. '91), then trained at Russian Academy of Sciences (Moscow) '93, before joining PhD programme in condensed matter physicist at the University of Utah, USA (completed 99). He has then joined Cavendish Laboratory, University of Cambridge, and later Merck Chemicals to work on organic semiconductors. Since 07, he has held a Lecturer in Nanoelectronics position at Advanced Technology Institute, Electrical and Electronic Engineering, University of Surrey, and led the development of large area printed electronics. His research targets the integration of nanomaterials in solution-processed electronics involving device nano-fabrication and processing, organic and inorganic nanoparticles self-assembly, characterisation of solution-processed semiconductors, nanomaterials ink-jet printing on rigid and flexible substrates as well as physics and engineering aspects of printed electronics. He has (co)-authored over 110 publications, including papers and patents.

Grigorios-Panagiotis Rigas received his BEng in Electronic and Computer Networks engineering from the Technical University of Piraeus (Greece). . In 2012 he obtained an MSc in Nanotechnology and Nanoelectronic Devices from the University of Surrey (UK) and in 2013, he joined University of Surrey for PhD in Electrical and Electronic Engineering, focusing on the development of novel manufacturing and characterization techniques for printed electronics. Grigorios (co-)authored more than 20 peer-reviewed papers and conference presentations in the field of printed electronics. His current research interests include the development of advanced manufacturing and characterization approaches for next generation biosensors and bioelectronics.

Paul Blanchard received the B.S. degree in engineering physics from the Colorado School of Mines, Golden, in 2005.

He is currently a Device Engineer and Physicist in the Quantum Electronics and Photonics Division, National Institute of Standards and Technology, Boulder, CO. His research interests include the characterization and modeling of nanowire material properties, nanoscale semiconductor contacts, and nanowire-based optoelectronic and FET devices.

Vijay Devabhaktuni (S'97-M'03-SM'09) received the B.Eng. degree in electronics and electrical engineering and the M.Sc. degree in physics from the Birla Institute of Technology Science, Pilani, India, in 1996, and the Ph.D. degree in electronics from Carleton University, Ottawa, ON, Canada, in 2003.

He held the Natural Sciences and Engineering Research Council of Canada Post-Doctoral Fellowship and spent the tenure researching with the University of Calgary, Calgary, AB, Canada, from 2003 to 2004. In 2005, he taught with Penn State Erie, The Behrend College University, Erie, PA, USA. From 2005 to 2008, he held the internationally prestigious Canada Research Chair in Computer-Aided High-Frequency Modeling and Design with Concordia University, Montreal, QC, Canada. In 2008, he joined the Department of Electrical Engineering and Computer Sciences, The University of Toledo, Toledo, OH, USA, as an Associate Professor. Since 2012, he has been the Director of the College of Engineering for Interdisciplinary Research Initiatives, where he has been recently promoted to Full Professor. He secured external funding close to U.S. 5 million in his research areas (sponsoring agencies include AFOSR, CFI, ODOT, NASA, NSERC, NSF, and industry). He has co-authored around 190 peer-reviewed papers and advises 13 M.S./Ph.D. students. His current research interests include applied electromagnetics, biomedical applications of wireless networks, computer aided design, device modeling, image processing, infrastructure monitoring, neural networks, optimization methods, power theft modeling and education, RF/microwave optimization, and virtual reality. Dr. Devabhaktuni is a Registered Member of the Association of Professional Engineers, Geologists and Geophysicists of Alberta. He received the Carleton University Senate Medal for his outstanding scholastic accomplishments at the Ph.D. level. He has received several teaching excellence awards in Canada and USA. He serves as the Associate Editor of the *International Journal of RF and Microwave Computer-Aided Engineering*.